Redox Biology 11 (2017) 118–125

Contents lists available at ScienceDirect

Redox Biology

journal homepage: www.elsevier.com/locate/redox

Research Paper

NOX isoforms in the development of abdominal aortic aneurysm

Kin Lung Siu[a,1], Qiang Li[a,1], Yixuan Zhang[a], Jun Guo[b], Ji Youn Youn[a], Jie Du[b], Hua Cai[a,*]

[a] Divisions of Molecular Medicine and Cardiology, Departments of Anesthesiology and Medicine, Cardiovascular Research Laboratories, David Geffen School of Medicine at University of California Los Angeles, 650 Charles E. Young Drive, Los Angeles, CA 90095, USA

[b] Beijing Anzhen Hospital, Capital Medical University, The Key Laboratory of Remodeling-Related Cardiovascular Diseases, Ministry of Education, Beijing Collaborative Innovation Center for Cardiovascular Disorders, Beijing Institute of Heart, Lung & Blood Vessel Disease, Beijing 100029, China

ARTICLE INFO

Keywords:
Abdominal aortic aneurysms (AAA)
Angiotensin II (Ang II)
Nicotinamide adenine dinucleotide phosphate oxidase (NADPH oxidase/NOX)
NOX1
NOX2
NOX4
p47phox
Endothelial nitric oxide synthase (eNOS) uncoupling
Dihydrofolate reductase (DHFR)
Superoxide
Tetrahydrobiopterin (H_4B)
Nitric oxide (NO)

ABSTRACT

Oxidative stress plays an important role in the formation of abdominal aortic aneurysm (AAA), and we have recently established a causal role of uncoupled eNOS in this severe human disease. We have also shown that activation of NADPH oxidase (NOX) lies upstream of uncoupled eNOS. Therefore, identification of the specific NOX isoforms that are required for eNOS uncoupling and AAA formation would ultimately lead to novel therapies for AAA. In the present study, we used the Ang II infused hph-1 mice to examine the roles of NOX isoforms in the development of AAA. We generated double mutants of hph-1-NOX1, hph-1-NOX2, hph-1-p47phox, and hph-1-NOX4. After two weeks of Ang II infusion, the incidence rate of AAA substantially dropped from 76.5% in Ang II infused hph-1 mice (n=34) to 11.1%, 15.0%, 9.5% and 0% in hph-1-NOX1 (n=27), hph-1-NOX2 (n=40), hph-1-p47phox (n=21), and hph-1-NOX4 (n=33) double mutant mice, respectively. The size of abdominal aortas of the four double mutant mice, determined by ultrasound analyses, was significantly smaller than the hph-1 mice. Aortic nitric oxide and H_4B bioavailabilities were markedly improved in the double mutants, while superoxide production and eNOS uncoupling activity were substantially diminished. These effects seemed attributed to an endothelial specific restoration of dihydrofolate reductase expression and activity, deficiency of which has been shown to induce eNOS uncoupling and AAA formation in both Ang II-infused hph-1 and apoE null animals. In addition, over-expression of human NOX4 N129S or T555S mutant newly identified in aneurysm patients increased hydrogen peroxide production, further implicating a relationship between NOX and human aneurysm. Taken together, these data indicate that NOX isoforms 1, 2 or 4 lies upstream of dihydrofolate reductase deficiency and eNOS uncoupling to induce AAA formation. These findings may promote development of novel therapeutics for the treatment of the disease by inhibiting NOX signaling.

1. Introduction

Abdominal aortic aneurysms (AAA) occur in adults older than 65 years old, and the number of deaths in U.S. attributed to ruptured AAAs increased from 99,600 in 1990 to 151,500 in 2013 [1,2]. One of the key features of AAA is vascular wall remodeling associated with significant production of reactive oxygen species (ROS) [3]. We have recently established a causal role of eNOS uncoupling in the formation of AAA [4,5,6]. Infusion of Ang II into hyperphenylalaninemia (hph)-1 mice induced a three-fold increase in the uncoupling activity of eNOS, resulting in 79% of AAA development within two weeks; and recoupling of eNOS by folic acid administration effectively inhibited the development of AAA [5,6]. Uncoupling of eNOS is also responsible for AAA formation in Ang II infused apoE null mice [4].

We have shown that NADPH oxidase (NOX) activation lies upstream of eNOS uncoupling in endothelial cells [7], diabetic mice [7], and ischemia/reperfusion-injured heart [9]. The NOX family members expressed in the cardiovascular system include NOX1, 2, 4, and 5 [10–13]. It seems that different NOX isoforms are involved in the pathogenesis of different cardiovascular disorders. For example, NOX1, but not NOX2 or NOX4, underlies endothelial dysfunction in streptozotocin-induced type 1 diabetes mellitus [15]. While protective laminar shear stress assembles NOX2-p47phox at basal levels to increase eNOS phosphorylation and nitric oxide (NO) production, atherogenic oscillatory shear stress activates NOX1-NOXO1 complex to uncouple eNOS and sustain oxidative stress [16]. On the other hand, NOX4 but not NOX1/2, is activated to mediate eNOS uncoupling in ischemia/reperfusion (I/R)-injured heart, and involved in cardiac damage and remodeling [9,17,18]. NOX4 upregulation also correlates with the presence of atrial fibrillation in patients, and promotes cardiac

* Corresponding author.
E-mail address: hcai@mednet.ucla.edu (H. Cai).
[1] The authors contribute equally to this work.

http://dx.doi.org/10.1016/j.redox.2016.11.002
Received 17 October 2016; Received in revised form 7 November 2016; Accepted 7 November 2016
Available online 19 November 2016
2213-2317/

arrhythmic phenotype in a zebrafish model [19,20]. In addition, it has been shown that NOX1/2 inhibition through genetic deletion of p47phox attenuated atherogenesis in young apoE null mice [21].

In the present study we examined effects on AAA formation of genetic deletion of different NOX isoforms. Hph-1 mice were crossed with NOX1, NOX2, p47phox, and NOX4 knockout mice to generate double mutants. Inhibition of any NOX isoforms or p47phox significantly reduced the incidence of AAA while abolishing pathophysiological features. This was associated with restored eNOS coupling activity. Two human NOX4 mutants N129S and T555S newly identified in aneurysm patients had increased H_2O_2 production. These data suggest that inhibition of NOX signaling may prove to be an effective therapeutic strategy for aortic aneurysms.

2. Methods

2.1. Reagents

Unless otherwise noted, all chemicals were purchased from Sigma-Aldrich (St Louis, MO, USA) in the highest purity. Isoflurane was obtained from Piramal Healthcare (Bethlehem, PA, USA). Heparin sodium injection solution was from Sagent Pharmaceuticals (Schaumburg, IL, USA).

2.2. Production of double mutant animals

All animals and experimental procedures were approved by the Institutional Animal Care and Usage Committee at the University of California, Los Angeles. Homozygote hph-1 mice were maintained as described before [5,6]. NOX1-null founder mice were generously provided by Dr. Karl-Heinz Krause from the University of Geneva [22]. NOX2-null and p47phox-null founder mice were originally purchased from Jackson Laboratory (Bar Harbor, Maine, strain 002365 and 004742, respectively). NOX4-null founder mice were kindly provided by Dr. Junichi Sadoshima from the Rutgers University. Double mutants of NOX1, NOX2, p47phox, or NOX4 with hph-1 animals were generated in-house by breeding male NOX1, NOX2, p47phox, and NOX4 knockouts with female hph-1 animals. The pups were genotyped using PCR, and double mutants were used for all future breeding.

2.3. Genotyping of the double mutant animals

Genomic DNA was isolated from tail clips as per standard protocol, using protease K (Invitrogen, Carlsbad, CA, USA) to digest the tail, followed by elution of the DNA by isopropanol. For the NOX1 KO, the PCR primers used were: 5′-ACGGGCACA TGTGTAAGACTCACC-3′, 5′-GCCTGCAACTCCCCTTATGGTCA-3′, and 5′-CTACCAGGCCAATCTC-TCTGTTTCCA-3′. The PCR amplification was performed using the conditions of 95 °C for 5 min, followed by 34 cycles of 95 °C for 15 s, 61 °C for 15 s and 72 °C for 48 s. For the NOX2 KO, the PCR primers used were 5′-AAGAGAAACTCCTCTGCTGTGAA-3′, 5′-CGCACTGGAA-CCCCTGAGAAAGG-3′, 5′-GTTCTAATTCCATCAGAAGCTTATCG-3′. The PCR amplification was performed using the conditions of 95 °C for 15 min, followed by 35 cycles of 94 °C for 20 s, 58 °C for 60 s and 72 °C for 45 s. For the p47phox KO, the PCR primers used were : 5′-TGGAAGAAGCTGAGAGTTGAGG-3′ and 5′-TCCAGGAGCTTATGAAT-GACC-3′. The PCR amplification was performed using the conditions of 95 °C for 15 min, followed by 35 cycles of 94 °C for 30 s, 55 °C for 30 s and 72 °C for 30 s. For NOX4 KO , the PCR primers used were 5′-CATCTTCTTGTTTTTATCCAATTTAAATTTAG-3′ and 5′-GCAGATCT-CAAACACAGAATTAATCTG-3′. The PCR amplification was performed using the conditions of 95 °C for 3 min, followed by 30 cycles of 94 °C for 60 s, 50 °C for 60 s and 72 °C for 30 s. For the hph-1, the primers used were: 5′-AGGCTGCCCATAAAAGGG-3′ and 5′-GTTTGTGCTAA-TGTTCTCATCTGG-3′. The PCR amplification was performed using the conditions of 95 °C for 15 min, followed by 35 cycles of 94 °C for 20 s, 58 °C for 60 s and 72 °C for 45 s [5,6] .

2.4. Osmotic pump infusion of Ang II

Animals were anesthetized with isoflurane in an isoflurane chamber, and then moved to a nose cone supplying 1.5–2% isoflurane to maintain the anesthetic state. A small area between the shoulder blades in the back of the mice was removed of hair, and then disinfected with an iodine solution. A small incision was made at the site, followed by the insertion of an osmotic pump (Alzet, model 2002, Cupertino, CA, USA) containing Ang II (0.7 mg/kg/day) in a delivery solution (3.8 mL H_2O, 120 µl 5 M NaCl, 40 µl acetic acid) under the skin to the left flank. Surgical staples were used to close the site. The animals were placed in a heated chamber for recovery.

2.5. Ultrasound imaging of abdominal aorta

Animals were anesthetized (0.6–0.8% isoflurane in 95% oxygen, heart rate: 430–450 beats/min) with isoflurane and placed on a heated table that monitors electrocardiography (ECG). Heart rate was maintained above 400 bpm while keeping the animal sufficiently anesthetized (1.5–2% isoflurane). The hair in the abdomen was removed using a hair removal lotion (Veet, Reckitt Benckiser, Slough, United Kingdom). Pre-heated ultrasound transmission gel was applied over the cleaned abdomen area. An ultrasonic probe (Visualsonics 2100, MS400, 30 MHz. FUJIFILM VisualSonics, Inc. Toronto, Ontario, Canada) was placed onto the gel to visualize the abdominal aorta on the transverse plane. Doppler mode was used to detect pulsatile flow to confirm the location of the aorta. Consistent localization of the imaging area was ensured by imaging the aorta immediately superior to the left renal artery. For animals that have abdominal aneurysms, the measurement was made at the site of maximal aortic diameter.

2.6. Tissue collection

After 2 weeks of Ang II infusion, animals were euthanized with CO_2. The aortas were rapidly removed from the body, rinsed with ice cold modified Krebs/HEPES buffer (KHB: 99 mmol/L NaCl; 4.7 mmol/L KCl; 1.2 mmol/L $MgSO_4$; 1.0 mmol/L KH_2PO_4; 2.5 mmol/L $CaCl_2$; 25 mmol/L $NaHCO_3$; 5.6 mmol/L D-glucose; 20 mmol/L NaHEPES), and cleaned of connective tissue and fat on ice. Determination of AAA incidence was made using ultrasound measurement and/or inspection of the abdominal aorta post-mortem. A small section (about 2 mm) of the suprarenal aorta was removed for histology. This small section was fixed in 10% formalin overnight, followed by a 24 h incubation in 10% sucrose. The tissues were then embedded in paraffin and sliced at 5 µm.

2.7. Determination of aortic superoxide production using electron spin resonance

Aortic superoxide was measured by ESR as previously described [4,5,6,23,24]. Briefly, freshly isolated aortas were homogenized on ice in lysis buffer containing 1:100 protease inhibitor cocktail, and centrifuged at 12,000*g* for 15 min. Protein content of the supernatant was determined using a protein assay kit (Bio-Rad, Irvine, CA, USA). Five µg of protein was mixed with ice-cold and nitrogen bubbled Krebs/HEPES buffer containing diethyldithiocarbamic acid (5 µmol/L), deferoxamine (25 µmol/L), and the superoxide specific spin trap methoxycarbonyl-2,2,5,5-tetramethylpyrrolidine (CMH, 500 µmol/L, Axxora, San Diego, CA, USA). The mixture was then loaded into a glass capillary (Kimble, Dover, OH, USA), and assayed using the ESR spectrometer (eScan, Bruker, Billerica, MA, USA) for superoxide production. A second measurement was taken with the addition of PEG-SOD (100 U/mL) for the determination of background. For the assessment of eNOS uncoupling, a third measurement was made with

the addition of L-NAME (100 μmol/L). ESR settings used were: Center field, 3480; Sweep width, 9 G; microwave frequency, 9.78 GHz; microwave power, 21.02 mW; modulation amplitude, 2.47 G; 512 points of resolution; receiver gain, 1000.

2.8. Determination of aortic NO bioavailability using electron spin resonance

Aortic NO production was also measured using ESR as previous described [4,5,6,23,24]. Briefly, freshly isolated aortas were cut into 2 mm rings, and then incubated in freshly prepared NO specific spin trap trap $Fe^{2+}(DETC)_2$ (0.5 mmol/L) in nitrogen bubbled, modified Krebs/HEPES buffer (as described above) at 37°C for 60 min, in the presence of calcium ionophore A23187 (10 μmol/L). The aortic rings were then snap frozen in liquid nitrogen and loaded into a finger Dewar for measurement with ESR. The instrument settings were as the followings: Center field, 3440; Sweep width, 100 G; microwave frequency, 9.796 GHz; microwave power 13.26 mW; modulation amplitude, 9.82 G; 512 points of resolution; and receiver gain 356.

2.9. Determination of aortic H_4B bioavailability with HPLC

Aortic H_4B and its oxidized species were measured using HPLC as previously described [4,5,6,23,24]. Briefly, freshly isolated aortas were lysed in H_4B lysis buffer (0.1 mol/L phosphoric acid, 1 mmol/L EDTA, 10 mmol/L DL-Dithiothreitol), centrifuged at 12,000*g* for 3 min, and the lysates were subjected to differential oxidation in acidic (0.2 mol/L trichloroacetic acid with 2.5% I2 and 10% KI) and alkalytic (0.1 mol/L NaOH with 0.9% I2 and 1.5% KI) solutions. After centrifugation, 10 μl of the supernatant was injected into a HPLC system equipped with a fluorescent detector (SHIMADZU AMERICA INC, Carlsbad, CA, USA). Excitation and emission wavelengths of 350 nm and 450 nm were used to detect H_4B and its oxidized species. H_4B concentration was calculated as previously described [25,26].

2.10. Isolation of endothelial cells from aorta

Endothelial cells (ECs) were isolated from aortas as previously described [4,5,6]. Briefly, freshly isolated aortas were cut into small sections (about 2 mm) and digested in PBS containing collagenase (0.6 mg/mL) for 20 min at 37 °C. The aortic rings were then gently shaken in the digestion buffer to remove the ECs. The ECs were then collected via centrifugation at 1000*g* for 3 min at 4 °C. Both the denuded rings and ECs were lysed with lysis buffer for subsequent analyses of DHFR protein expression and activity.

2.11. Western blotting

Western blotting was performed as per standard protocols using 10% SDS/PAGE gels and transferring to nitrocellulose membranes. After 1 h blocking in PBS with 0.1% Tween-20 and 5% (w/v) non-fat dry milk, the membrane was then incubated with primary antibodies for DHFR (1:500, Novus Biologicals, Littleton, CO, USA), actin (1:3000, Sigma-aldrich, St Louis, MO, USA), and eNOS (1:2000, BD, Franklin Lakes, NJ, USA).

2.12. Determination of endothelial DHFR activity with HPLC

DHFR activity was measured from isolated EC or denuded aortic ring lysates as previously described [4,23]. Briefly, lysates were incubated in a DHFR assay buffer (0.1 mol/L potassium phosphate dibasic, 1 mmol/L DTT, 0.5 mmol/L KCl, 1 mmol/L EDTA, and 20 mmol/L sodium ascorbate at pH 7.4) with NADPH (200 μmol//L) and the substrate dihydrofolate (50 μmol/L) at 37 °C for 20 min in the dark. The product of the reaction, tetrahydrofolate (THF), was measured using a HPLC system (SHIMADZU AMERICA INC, Carlsbad, CA, USA) with a C-18 column (Alltech, Deerfield, MA, USA) using water based mobile phase consisting of 7% acetonitrile and 5 mmol/L of potassium phosphate dibasic at pH 2.3. The signal was detected using a fluorescent detector at 295 nm excitation and 365 nm emission. The THF content was calculated against a standard curve prepared by using THF solutions in assay buffer. Data are presented as nmol production of THF per min per mg protein.

2.13. Construction of NOX4 mutant plasmids

Full length coding region of human NOX4 (NM_016931, isoform A of human NOX4) in pCMV6-hNOX4 was purchased from OriGene (Rockville, MD, USA). Mutations of N129S, P437H and T555S were generated by PCR based site-directed mutagenesis (KOD Hot Start, Novagen, Darmstadt, Germany). All of the plasmids were confirmed by sequencing.

2.14. Determination of H_2O_2 Levels by Amplex Red Assay

HEK293T were cultured in media Dulbecco's Modified Eagle Medium (DMEM) containing 10% fetal bovine serum (FBS). One day after seeding in 60 mm dish, 6 μg of human NOX4 WT and mutant (P473H, N129S, and T555S) plasmids were transfected into HEK293T cells using lipofectamine 2000 as per manufacturer's instructions (Invitrogen, Carlsbad, CA, USA). Forty-eight hrs after transfection, cells were harvested in Krebs-Ringer buffer and mixed with Amplex Red reaction buffer as previously described [9]. Each sample was treated with or without PEG-catalase (100 U/mL). The samples were incubated at 37°C for 1 h in the dark, and then centrifuged at 2,500*g* for 5 min. The supernatants were loaded to a 96 well plate, and then measured using a BioTek fluorescent plate reader at 530 nm excitation and 590 nm emission respectively. Freshly prepared H_2O_2 standards were used to calculate the amount of H_2O_2 produced by the samples.

2.15. Statistical analysis

All statistical analysis was carried out with the Prism software. Comparisons between multiple groups are done using the one-way ANOVA test with a statistical threshold of 0.05, followed by the Newman-Keuls post-hoc test. Comparisons of the incidence rates were done using a contingency table, also with a statistical threshold of 0.05.

3. Results

3.1. Genetic knockout of NOX1, NOX2, p47phox, or NOX4 prevented AAA development in Ang II infused hph-1 mice

We firstly crossed hph-1 mice with NOX1, NOX2, p47phox, or NOX4 knockout mice to generate new double mutant mice. To investigate the role of NOX signaling in AAA formation, these mice were infused with Ang II for two weeks. In the hph-1 group, 76.5% of the animals developed AAA, which is comparable to our previous reports [5,6]. In contrast, only 11.1%, 15.0%, and 0% of the animals developed AAA in hph-1-NOX1, hph-1-NOX2, and hph-1-NOX4 double mutant mice group respectively (Fig. 1). Moreover, hph-1 animals that also have p47phox (a cytosolic regulatory subunit of NOX1 and NOX2 [21]) deficiency developed AAA in 9.5% of the animals received Ang II infusion. These data suggest that activation of NOX isoforms is involved in Ang II induced AAA formation in hph-1 mice.

3.2. NOX1, NOX2, p47phox, or NOX4 knockout inhibited abdominal aortic expansion and abolished extensive medial elastin breakdown and adventitial remodeling in Ang II infused hph-1 mice

Ultrasound images were taken to examine the size of the abdominal

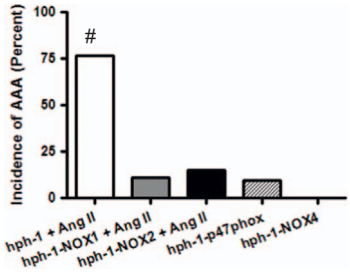

	AAA	No AAA
hph-1 + Ang II	26	8
hph-1-NOX1 + Ang II	3	24
hph-1-NOX2 + Ang II	6	34
hph-1-p47phox + AngII	2	19
hph-1-NOX4 + AngII	0	33

Fig. 1. NOX1, NOX2, p47phox, or NOX4 knockout greatly reduced the incidence of AAA in Ang II-infused hph-1 mice. The top panel shows the percentage of AAA in each strain of mice subjected to Ang II infusion, while the bottom panel shows the actual numbers of animals for each group. The incidence of AAA was greatly reduced from 76.5% in AngII-infused hph-1 animals to 11.1%, 15.0%, 9.5% and 0% in hph-1-NOX1, hph-1-NOX2, hph-1-p47phox, and hph-1-NOX4 double mutant animals, respectively. $^{\#}p < 0.001$.

aortas in the double mutant animals before Ang II infusion and at the end of the 2 week infusion. Ang II infusion for two weeks resulted in significant expansion of abdominal aortas (Fig. 2). However, the abdominal aortas of hph-1-NOX1, hph-1-NOX2, hph-1-p47phox, and hph-1-NOX4 double mutant animals were substantially smaller than those of hph-1 alone (hph-1-NOX1 with Ang II: 1.31 ± 0.08 mm^2, hph-1-NOX2 with Ang II: 1.44 ± 0.08 mm^2, hph-1-p47phox with Ang II: 1.60 ± 0.24 mm^2, hph-1-NOX4 with Ang II: 1.38 ± 0.06 mm^2 vs. hph-1 with Ang II: 3.12 ± 0.27 mm^2, $p < 0.001$). Moreover, as shown in Fig. 3, H & E staining from the abdominal aortic sections demonstrated that Ang II infusion led to dramatic medial elastin fiber breakdown and adventitial hypertrophy in hph-1 mice, which were largely absent in hph-1-NOX1, hph-1-NOX2, hph-1-p47phox, and hph-1-NOX4 double mutant animals. These results confirmed that inhibition of NOX signaling might be an effective approach to attenuate AAA formation.

3.3. NOX1, NOX2, p47phox, or NOX4 knockout improved NO and H_4B bioavailabilities, reduced superoxide production, and recoupled eNOS in Ang II infused hph-1 mice

Our previous studies have established a novel causal role of eNOS uncoupling in AAA formation [4,5,6,23,24]. In addition, there are evidences that Ang II transiently activates NOXs, resulting in uncoupling of eNOS in endothelial cells [7,8]. To explore the mechanisms whereby NOX signaling mediates AAA formation, we firstly measured

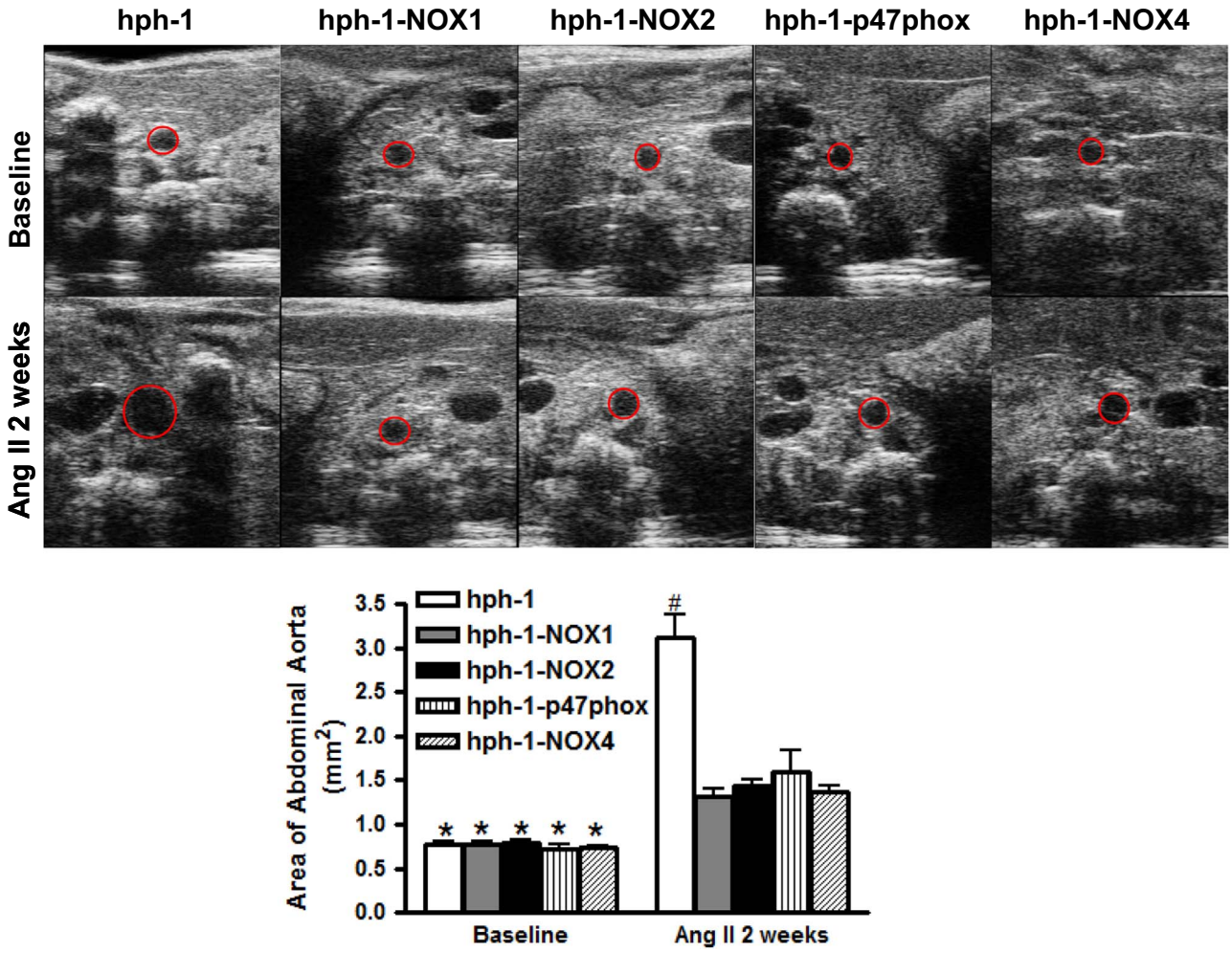

Fig. 2. Hph-1-NOX1, hph-1-NOX2, hph-1-p47phox, and hph-1-NOX4 double mutant mice had inhibited abdominal aortic expansion in response to Ang II. Representative ultrasound images (top panel) and grouped data (bottom panel) of abdominal aortas of Ang II-infused animals. The prominent expansion of the abdominal aorta observed in the Ang II-infused hph-1 animals was substantially attenuated in hph-1-NOX1, hph-1-NOX2, hph-1-p47phox, and hph-1-NOX4 double mutant mice, n=5–9, $^{*}p < 0.05$, $^{\#}p < 0.001$.

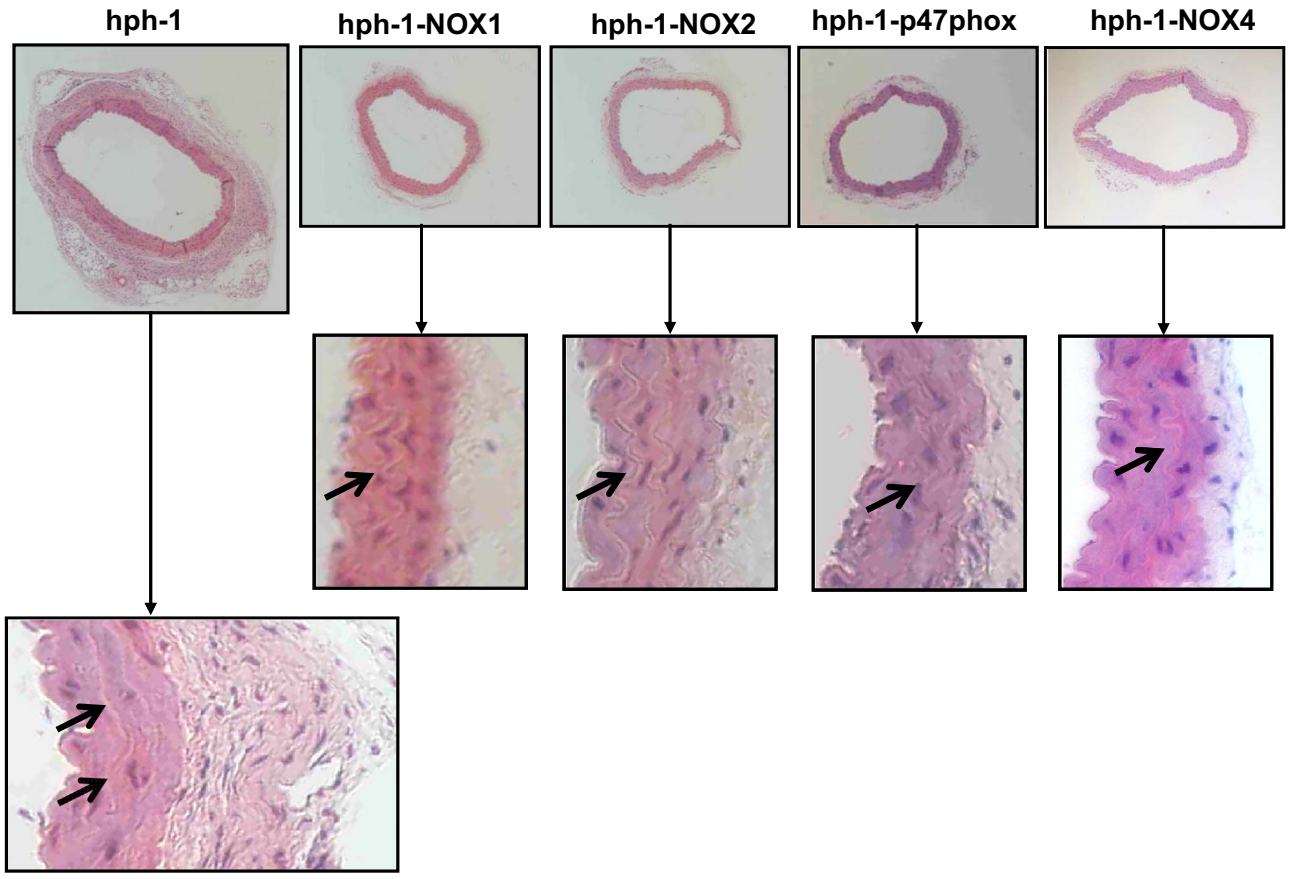

Fig. 3. The extensive elastin breakdown and adventitial remodeling of the abdominal aorta in AngII-infused hph-1 mice was substantially attenuated in hph-1-NOX1, hph-1-NOX2, hph-1-p47phox, and hph-1-NOX4 double mutant mice. Shown are representative histological images of the abdominal aortas from Ang II infused hph-1, hph-1-NOX1, hph-1-NOX2, hph-1-p47phox, and hph-1-NOX4 animals. The results show that the breakdown of the elastin fibers and enlargement of the adventitial layer in the abdominal aortas of the AngII-infused hph-1 animals were eliminated in the hph-1-NOX1, hph-1-NOX2 and hph-1-p47phox, and hph-1-NOX4 animals.

aortic NO production from different double mutants infused of Ang II for 2 weeks. The results show that these four strains of double knockouts had significantly improved NO production (Fig. 4A), and it was recovered back to the similar level in hph-1 mice without Ang II infusion as observed previously [5].

Aortic superoxide production with or without L-NAME, which is an inhibitor of NOS activity, was further measured using ESR. The white bars in Fig. 4B show that all four strains of the double mutants had reduced superoxide production compared to Ang II infused hph-1 animals, and this is to the baseline in hph-1 mice without Ang II infusion as previously reported [5]. L-NAME was used to assess the coupling state of eNOS. When eNOS is coupled and functional, the addition of L-NAME will inhibit NO and increase superoxide. However, if eNOS is uncoupled and producing superoxide, the addition of L-NAME will reduce total superoxide production. Therefore, the relative change between the two measurements shows the coupling state of eNOS of the sample. The L-NAME measurements are shown as black bars in Fig. 4B. For hph-1 animals under Ang II infusion, the addition of L-NAME greatly reduced superoxide production, which suggests uncoupling of eNOS as observed previously [5]. The addition of L-NAME to the aortic samples of double mutants, however, resulted in very little change in superoxide production, suggesting almost complete recoupling of eNOS in these groups.

To further examine the coupling state of eNOS, H_4B, the critical cofactor that determines the coupling/uncoupling switch of eNOS, was measured from the aortas of animals after 2 weeks of Ang II infusion, which led to H_4B reduction in hph-1 mice at baseline (1.87 ± 0.25 pmol/mg protein to 0.99 ± 0.11 pmol/mg) [5]. The results in Fig. 4C showed that aortas from the four double mutants had significantly higher H_4B levels compared to hph-1s alone, suggesting an improvement in the coupling state of eNOS in these animals. This recovery is complete (~2 pmol/mg protein) to the baseline in hph-1 mice without Ang II infusion as documented previously and described above [5]. Therefore, these data confirmed that NOX isoforms take part in the regulation of eNOS coupling state to mediate AAA formation.

3.4. Double mutant of hph-1 with NOX1, NOX2, p47phox, or NOX4 had preserved endothelial specific DHFR expression and activity in response to Ang II infusion

Our previous studies have shown that the reduction of H_4B in Ang II infused hph-1 and apoE null mice is consequent to an endothelial specific deficiency in DHFR, a salvage enzyme for H_4B [4,5,6]. Here, we examined whether the improvement in H_4B levels in the double mutant mice was a result of improved endothelial DHFR function. We first measured DHFR protein levels in isolated aortic endothelial cells (ECs) and EC-denuded aortic rings from mutant mice infused with Ang II. As shown in Fig. 5A–C, eNOS was detected only in the fractions of ECs, but not in the EC-denuded aortic rings. The DHFR protein abundance in the ECs of the four double mutant mice was significantly higher than those of hph-1s that displayed an EC-specific deficiency (5), while no significant changes were observed in the EC-denuded rings. In addition, data on DHFR activities mirrored the responses of DHFR protein expression (Fig. 5D). These results demonstrated an intermediate role of endothelial specific DHFR deficiency in NOX isoform-dependent eNOS uncoupling and consequent AAA formation.

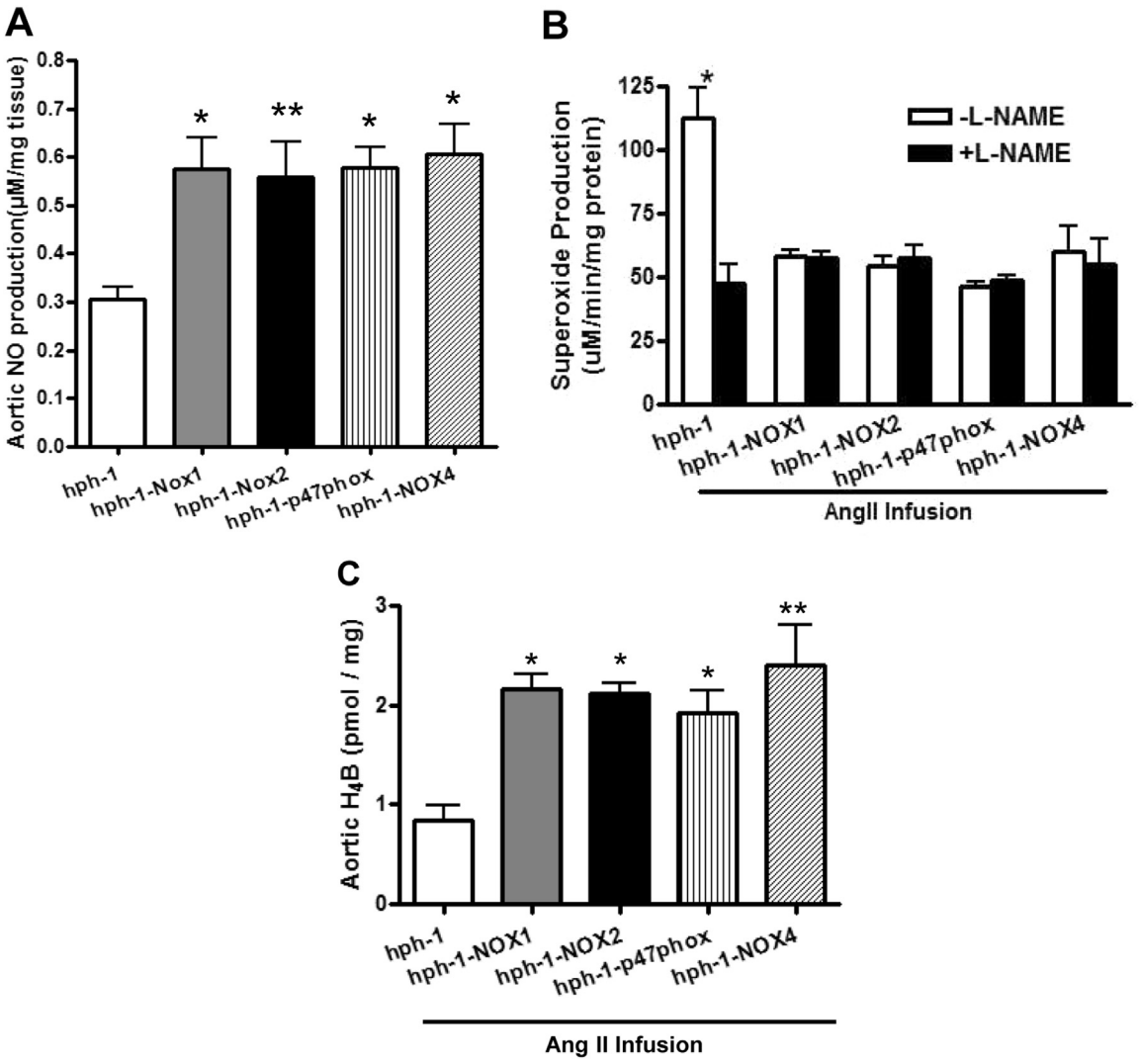

Fig. 4. NOX1, NOX2, p47phox, or NOX4 knockout improved NO and H_4B bioavailabilities, reduced superoxide production, and recoupled eNOS in Ang II infused hph-1 mice. **(A)** Aortic nitric oxide (NO) production was determined from aortic segments using electron spin resonance (ESR). Double mutants of hph-1 with NOX1, NOX2, p47phox, or NOX4 corrected the decline in aortic NO production in Ang II-infused hph-1 animals. n=4, *$p < 0.05$, **$p < 0.01$. **(B)** Total superoxide production was measured from aortic homogenates using ESR. eNOS uncoupling activity was assessed by comparing measurements with and without the addition of L-NAME, a NOS inhibitor, n=4–7, *$p < 0.05$. A reduction in superoxide production with L-NAME indicates that NOS is uncoupled and producing superoxide. The eNOS uncoupling phenotype in hph-1 mice was prevented in all of the double mutant mice. **(C)** Aortic H_4B bioavailability was determined by HPLC, and the deficiency of H_4B in hph-1 mice was corrected in all of the double mutant mice. n=5, *$p < 0.05$, **$p < 0.01$.

3.5. Two human NOX4 mutants N129S and T555S identified in aneurysm patients had increased H_2O_2 production

In an effort to screen for genetic variants in aneurysm patients (Supplemental for detailed methods), we have identified 2 novel mutants in NOX4 gene, N129S and T555S. N129S locates in the extracellular loop between the transmembrane domains III and IV. T555S locates in the cytoplasmic COOH terminus. We next generated WT NOX4, P437H (dominate negative mutation for NADPH binding), N129S, and T555S mutant plasmids, and transfected into HEK293T cells. Productions of H_2O_2 from these cells were determined using Amplex Red Assay (Fig. 6). The increased H_2O_2 production induced by human WT NOX4 overexpression, was effectively blocked in the P437H mutant group (P437H: 0.87 ± 0.24 nmole/mg protein vs. hNOX4: 2.84 ± 0.43 nmole/mg protein, $p < 0.05$) Of note, both N129S and T555S mutations resulted in marked increase in H_2O_2 production compared to the WT group (N129S: 5.25 ± 0.94 nmole/mg protein vs. hNOX4, $p < 0.01$; T555S: 4.65 ± 0.64 nmole/mg protein vs. hNOX4, $p < 0.05$). Taken together, these data indicate that two human NOX4 mutants N129S and T555S might be involved in aneurysm development through producing more H_2O_2, which functions as an intermediate to induce endothelial DHFR deficiency and eNOS uncoupling [7].

4. Discussion

In the present study, we examined the role of the different isoforms of NOX in AAA formation in Ang II infused hph-1 mice. Genetic knockout of NOX1, NOX2, p47phox, or NOX4 in hph-1 animals prevented formation of AAA, reflected in reduced abdominal aortic expansion and recovery of extensive elastin breakdown and adventitial remodeling. Furthermore, the double mutant mice had improved aortic NO production and reduced superoxide production, due to restored eNOS coupling activity, which is consequent to the endothelial specific improvement in DHFR protein abundance and activity. In addition, human NOX4 mutations N129S and T555S producing more H_2O_2 might be the reason for aneurysm development in some patients. These findings establish NOX isoforms as novel targets for the treatment of aortic aneurysms.

NOXs are one of the major sources of oxidative stress in the blood vessels. Different isoforms separately or together display different functions. NOX1 has been shown to be involved in diabetic endothelial dysfunction and endothelial cell response to atherogenic oscillatory shear stress [15,16]. On the contrary, NOX4 plays a critical role in

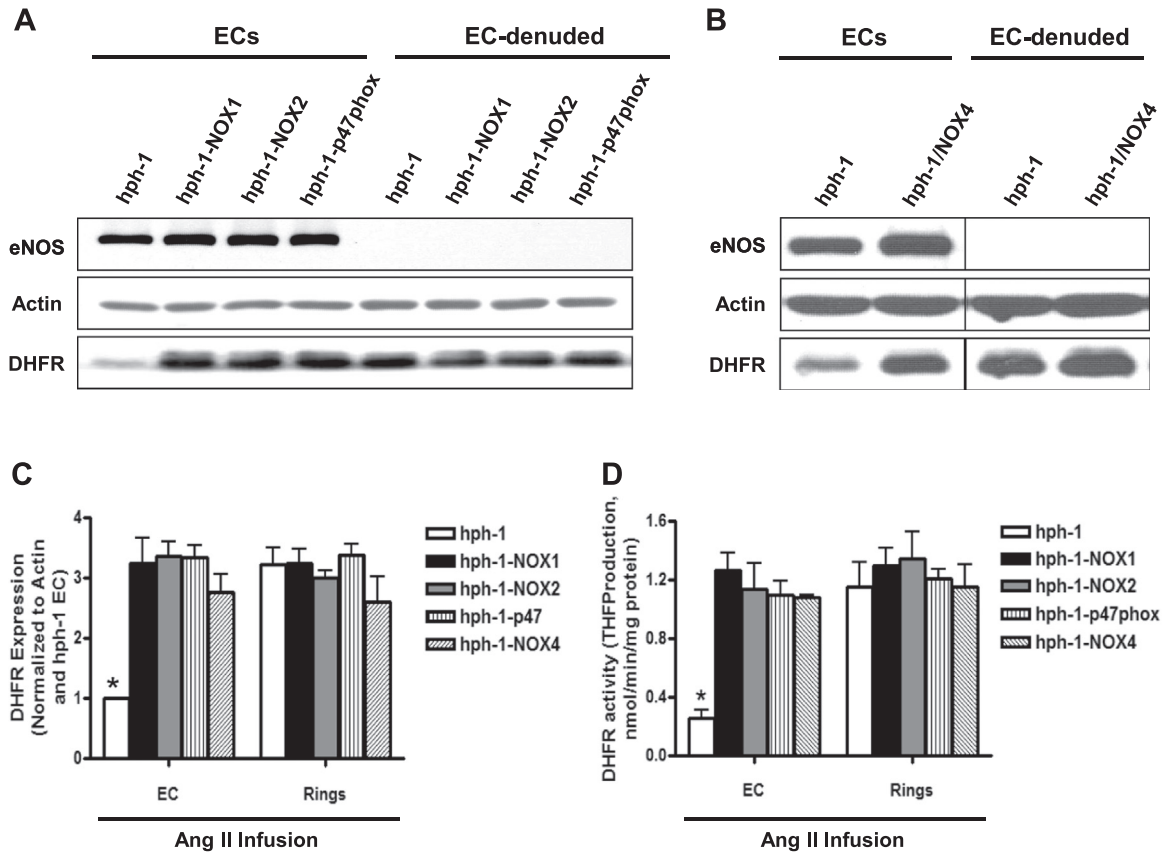

Fig. 5. NOX1, NOX2, p47phox, or NOX4 knockout markedly improved endothelial DHFR protein expression and activity in Ang II-infused hph-1 mice. **(A-B)** Representative Western blots of DHFR, actin, and eNOS from aortic endothelial cells (ECs) and EC-denuded aortas of Ang II-infused hph-1, hph-1-NOX1, hph-1-NOX2, hph-1-p47phox, and hph-1-NOX4 animals; **(C)** Grouped quantitative data of A-B, n=3, *p < 0.05. **(D)** DHFR activities measured from isolated aortic ECs and the EC-denuded aortas, n=3–5, *p < 0.05.

cardiac I/R injury [9]. Therefore, these isoforms are not functionally redundant. In the condition of Ang II infusion, NOX2 plays a major role in mediating Ang II-induced cerebral endothelial dysfunction [27]. However, both NOX1 and NOX2 were found involved in Ang II induced hypertension [28–31].

We have recently established a novel mouse model of AAA that has a high incidence rate of 79% two weeks post Ang II infusion into hph-1 mice [5,6]. Approximately 14% of the animals died of ruptured aneurysms within the short period of two weeks. This model is therefore associated with high morbidity and mortality. It is more severe than other currently known models, such as apoE null and LDLR null mice that require four weeks of Ang II infusion to develop aneurysms, and the animals do not die of ruptured aneurysms during the study period [4,32,33]. In the hph-1 model, Ang II induced more than a threefold increase in eNOS uncoupling activity. Our recent work also showed that NOX4 activation precedes eNOS uncoupling in I/R injured heart [8]. In addition, NOX activity has been implicated in AAA generation [34–37]. Therefore, in this study, we prefer to use this new model to investigate whether NOX isoforms are involved in the formation of AAA. Indeed, deletion of NOX1, NOX2, p47phox, or NOX4 conferred a protective effect against AAA formation in Ang II infused hph-1 mice.

Our result is consistent with previous findings that deletion of p47phox attenuates Ang II-induced AAA formation in apoE null mice [37]. As a cytosolic regulatory subunit, p47phox is required for the activation of both NOX1 and NOX2 [15,21,38,39]. Therefore, p47phox deletion also means inactivation of NOX1 and NOX2, which resulted in even more potent prevention of AAA formation. Although previous studies have mostly revealed a role of NOX4 in cardiac diseases [9,17–19], our data for the first time demonstrated an important role of NOX4 in Ang II induced AAA development. It turns out inhibition of

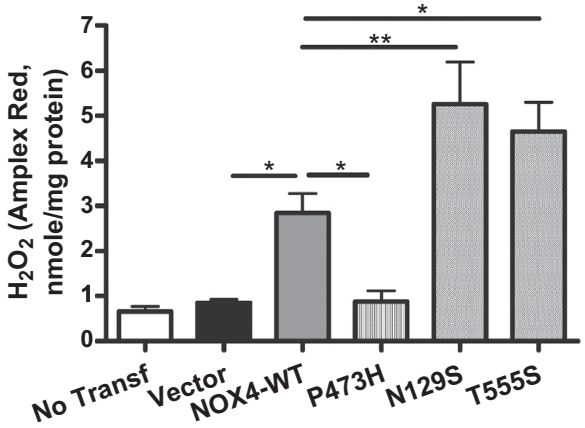

Fig. 6. Two human NOX4 mutants N129S and T555S identified in aneurysm patients had increased H_2O_2 production. Whole-exome sequencing was performed in Chinese Han patients with aneurysm. Through variants evaluation and Sanger sequencing, two human NOX4 mutants N129S and T555S were identified. NOX4 mutations of N129S and T555S, as well as the kinase inactive form of P437H with deficiency in NADPH binding, were generated by PCR based site-directed mutagenesis. HEK293T cells were transfected with indicated plasmids. Forty eight hrs later, cells were harvested for determination of for H_2O_2 production using the Amplex Red assay. n=4, *p < 0.05, **p < 0.01.

any of the NOX isoforms attenuates AAA by recoupling of eNOS, characterized by improved aortic NO and H_4B bioavailabilities and reduced superoxide production (Fig. 4). Indeed, the extent of eNOS uncoupling but not just the state, dictates the development of AAA, because eNOS is uncoupling at baseline in hph-1 mice which is

however well compensated, and Ang II infusion induces a threefold increase in eNOS uncoupling activity [5,6]. Therefore, recoupling of eNOS could represent an effective therapeutic approach for AAA following NOX inhibition, as afforded by oral folic acid administration [5,40]. The potential interactions among different NOX isoforms in the pathogenesis of AAA is of particular interest for future investigation.

In conclusion, in this study we examined the role of NOX isoforms in AAA using Ang II infused hph-1 mice. Animals that had the double mutant of hph-1 and NOX1, NOX2, p47phox or NOX4 had reduced AAA incidence and abdominal aortic expansion after Ang II infusion. Further, the double mutant animals had reduced superoxide production, improved NO and H_4B bioavailabilities, and restored eNOS coupling activity compared to hph-1 mice, and this effect is consequent to preserved DHFR function in the endothelium. Moreover, two NOX4 mutants existing in aneurysm patients (N129S and T555S) had increased H_2O_2 production. These findings prove that restoration of eNOS coupling activity by the inhibition of NOX signaling may serve as a novel therapeutic strategy for the management of AAA.

Disclosures

No conflicts of interest, financial or otherwise, are declared by the author(s).

Acknowledgements

This study was supported by National Institute of Health National Heart, Lung and Blood Institute (NHLBI) Grants HL077440 (HC), HL088975 (HC), HL108701 (HC, DGH), HL119968 (HC), an American Heart Association Established Investigator Award (EIA) 12EIA8990025 (HC) and an AHA Postdoctoral Fellowship Award 14POST20380966 (QL).

Appendix A. Supporting information

Supplementary data associated with this article can be found in the online version at doi:10.1016/j.redox.2016.11.002.

References

[1] N.L. Weintraub, Understanding abdominal aortic aneurysm, New Engl. J. Med. 361 (2009) 1114–1116.
[2] M. Writing Group, D. Mozaffarian, E.J. Benjamin, A.S. Go, D.K. Arnett, M.J. Blaha, et al., Heart disease and stroke statistics-2016 update: a report from the American Heart Association, Circulation 133 (2016) (e38-360).
[3] T.I. Emeto, J.V. Moxon, M. Au, J. Golledge, Oxidative stress and abdominal aortic aneurysm: potential treatment targets, Clin. Sci. 130 (2016) 301–315.
[4] K.L. Siu, X.N. Miao, H. Cai, Recoupling of eNOS with folic acid prevents abdominal aortic aneurysm formation in angiotensin II-infused apolipoprotein E null mice, PLoS One 9 (2014) e88899.
[5] L. Gao, K.L. Siu, K. Chalupsky, A. Nguyen, P. Chen, N.L. Weintraub, et al., Role of uncoupled endothelial nitric oxide synthase in abdominal aortic aneurysm formation: treatment with folic acid, Hypertension 59 (2012) 158–166.
[6] X.N. Miao, K.L. Siu, H. Cai, Nifedipine attenuation of abdominal aortic aneurysm in hypertensive and non-hypertensive mice: mechanisms and implications, J. Mol. Cell. Cardiol. 87 (2015) 152–159.
[7] K. Chalupsky, H. Cai, Endothelial dihydrofolate reductase: critical for nitric oxide bioavailability and role in angiotensin II uncoupling of endothelial nitric oxide synthase, Proc. Natl. Acad. Sci. USA 102 (2005) 9056–9061.
[8] J.H. Oak, H. Cai, Attenuation of angiotensin II signaling recouples eNOS and inhibits nonendothelial NOX activity in diabetic mice, Diabetes 56 (2007) 118–126.
[9] K.L. Siu, C. Lotz, P. Ping, H. Cai, Netrin-1 abrogates ischemia/reperfusion-induced cardiac mitochondrial dysfunction via nitric oxide-dependent attenuation of NOX4 activation and recoupling of NOS, J. Mol. Cell. Cardiol. 78 (2015) 174–185.
[10] B. Lassegue, A. San Martin, K.K. Griendling, Biochemistry, physiology, and pathophysiology of NADPH oxidases in the cardiovascular system, Circ. Res. 110 (2012) 1364–1390.
[11] H. Cai, NAD(P)H oxidase-dependent self-propagation of hydrogen peroxide and vascular disease, Circ. Res. 96 (2005) 818–822.
[12] H. Cai, Hydrogen peroxide regulation of endothelial function: origins, mechanisms, and consequences, Cardiovasc. Res. 68 (2005) 26–36.
[13] H. Cai, K.K. Griendling, D.G. Harrison, The vascular NAD(P)H oxidases as therapeutic targets in cardiovascular diseases, Trends Pharmacol. Sci. 24 (2003) 471–478.
[14] D.I. Brown, K.K. Griendling, Regulation of signal transduction by reactive oxygen species in the cardiovascular system, Circ. Res. 116 (2015) 531–549.
[15] J.Y. Youn, L. Gao, H. Cai, The p47phox- and NADPH oxidase organiser 1 (NOXO1)-dependent activation of NADPH oxidase 1 (NOX1) mediates endothelial nitric oxide synthase (eNOS) uncoupling and endothelial dysfunction in a streptozotocin-induced murine model of diabetes, Diabetologia 55 (2012) 2069–2079.
[16] K.L. Siu, L. Gao, H. Cai, Differential roles of protein complexes NOX1-NOXO1 and NOX2-p47phox in mediating endothelial redox responses to oscillatory and unidirectional laminar shear stress, J. Biol. Chem. 291 (2016) 8653–8662.
[17] J. Kuroda, T. Ago, S. Matsushima, P. Zhai, M.D. Schneider, J. Sadoshima, NADPH oxidase 4 (Nox4) is a major source of oxidative stress in the failing heart, Proc. Natl. Acad. Sci. USA 107 (2010) 15565–15570.
[18] S. Matsushima, H. Tsutsui, J. Sadoshima, Physiological and pathological functions of NADPH oxidases during myocardial ischemia-reperfusion, Trends Cardiovasc. Med. 24 (2014) 202–205.
[19] Y. Zhang, H. Shimizu, K.L. Siu, A. Mahajan, J.N. Chen, H. Cai, NADPH oxidase 4 induces cardiac arrhythmic phenotype in zebrafish, J. Biol. Chem. 289 (2014) 23200–23208.
[20] J. Zhang, J.Y. Youn, A.Y. Kim, R.J. Ramirez, L. Gao, D. Ngo, et al., NOX4-dependent hydrogen peroxide overproduction in human atrial fibrillation and HL-1 atrial cells: relationship to hypertension, Front. Physiol. 3 (2012) 140.
[21] P.A. Barry-Lane, C. Patterson, M. van der Merwe, Z. Hu, S.M. Holland, E.T. Yeh, et al., p47phox is required for atherosclerotic lesion progression in ApoE(−/−) mice, J. Clin. Investig. 108 (2001) 1513–1522.
[22] G. Gavazzi, B. Banfi, C. Deffert, L. Fiette, M. Schappi, F. Herrmann, et al., Decreased blood pressure in NOX1-deficient mice, FEBS Lett. 580 (2006) 497–504.
[23] L. Gao, K. Chalupsky, E. Stefani, H. Cai, Mechanistic insights into folic acid-dependent vascular protection: dihydrofolate reductase (DHFR)-mediated reduction in oxidant stress in endothelial cells and angiotensin II-infused mice: a novel HPLC-based fluorescent assay for DHFR activity, J. Mol. Cell. Cardiol. 47 (2009) 752–760.
[24] J.Y. Youn, J. Zhou, H. Cai, Bone morphogenic protein 4 mediates NOX1-dependent eNOS uncoupling, endothelial dysfunction, and COX2 induction in type 2 diabetes mellitus, Mol. Endocrinol. 29 (2015) 1123–1133.
[25] N.J. Alp, S. Mussa, J. Khoo, S. Cai, T. Guzik, A. Jefferson, et al., Tetrahydrobiopterin-dependent preservation of nitric oxide-mediated endothelial function in diabetes by targeted transgenic GTP-cyclohydrolase I overexpression, J. Clin. Investig. 112 (2003) 725–735.
[26] S. Cai, N.J. Alp, D. McDonald, I. Smith, J. Kay, L. Canevari, et al., GTP cyclohydrolase I gene transfer augments intracellular tetrahydrobiopterin in human endothelial cells: effects on nitric oxide synthase activity, protein levels and dimerisation, Cardiovasc. Res. 55 (2002) 838–849.
[27] S. Chrissobolis, B. Banfi, C.G. Sobey, F.M. Faraci, Role of Nox isoforms in angiotensin II-induced oxidative stress and endothelial dysfunction in brain, J. Appl. Physiol. 113 (2012) 184–191.
[28] K. Matsuno, H. Yamada, K. Iwata, D. Jin, M. Katsuyama, M. Matsuki, et al., Nox1 is involved in angiotensin II-mediated hypertension: a study in Nox1-deficient mice, Circulation 112 (2005) 2677–2685.
[29] H.D. Wang, S. Xu, D.G. Johns, Y. Du, M.T. Quinn, A.J. Cayatte, et al., Role of NADPH oxidase in the vascular hypertrophic and oxidative stress response to angiotensin II in mice, Circ. Res. 88 (2001) 947–953.
[30] G.R. Drummond, C.G. Sobey, Endothelial NADPH oxidases: which NOX to target in vascular disease?, Trends Endocrinol. Metab.: TEM 25 (2014) 452–463.
[31] U. Landmesser, H. Cai, S. Dikalov, L. McCann, J. Hwang, H. Jo, et al., Role of p47(phox) in vascular oxidative stress and hypertension caused by angiotensin II, Hypertension 40 (2002) 511–515.
[32] A. Daugherty, M.W. Manning, L.A. Cassis, Angiotensin II promotes atherosclerotic lesions and aneurysms in apolipoprotein E-deficient mice, J. Clin. Investig. 105 (2000) 1605–1612.
[33] L.A. Cassis, M. Gupte, S. Thayer, X. Zhang, R. Charnigo, D.A. Howatt, et al., ANG II infusion promotes abdominal aortic aneurysms independent of increased blood pressure in hypercholesterolemic mice, Am. J. Physiol. Heart Circ. Physiol. 296 (2009) H1660–H1665.
[34] F.J. Miller Jr., W.J. Sharp, X. Fang, L.W. Oberley, T.D. Oberley, N.L. Weintraub, Oxidative stress in human abdominal aortic aneurysms: a potential mediator of aneurysmal remodeling, Arterioscler. Thromb. Vasc. Biol. 22 (2002) 560–565.
[35] B. Guzik, A. Sagan, D. Ludew, W. Mrowiecki, M. Chwala, B. Bujak-Gizycka, et al., Mechanisms of oxidative stress in human aortic aneurysms–association with clinical risk factors for atherosclerosis and disease severity, Int. J. Cardiol. 168 (2013) 2389–2396.
[36] W. Xiong, J. Mactaggart, R. Knispel, J. Worth, Z. Zhu, Y. Li, et al., Inhibition of reactive oxygen species attenuates aneurysm formation in a murine model, Atherosclerosis 202 (2009) 128–134.
[37] M. Thomas, D. Gavrila, M.L. McCormick, F.J. Miller Jr., A. Daugherty, L.A. Cassis, et al., Deletion of p47phox attenuates angiotensin II-induced abdominal aortic aneurysm formation in apolipoprotein E-deficient mice, Circulation 114 (2006) 404–413.
[38] D.G. Harrison, H. Cai, U. Landmesser, K.K. Griendling, Interactions of angiotensin II with NAD(P)H oxidase, oxidant stress and cardiovascular disease, J. Renin-Angiotensin-Aldosterone Syst.: JRAAS 4 (2003) 51–61.
[39] M.R. DiStasi, J.L. Unthank, S.J. Miller, Nox2 and p47(phox) modulate compensatory growth of primary collateral arteries, Am. J. Physiol. Heart Circ. Physiol. 306 (2014) H1435–H1443.
[40] Q. Li, J.Y. Youn, H. Cai, Mechanisms and consequences of endothelial nitric oxide synthase dysfunction in hypertension, J. Hypertens. 33 (2015) 1128–1136.